Kinetic Investigation of Chemical Vapor Deposition of B_4C on Tungsten Substrate

Mustafa Karaman, N. Aslı Sezgi, Timur Doğu, and H. Önder Özbelge
Dept. of Chemical Engineering, Middle East Technical University, 06531, Ankara, Turkey

DOI 10.1002/aic.11017

Production of β-rhombohedral boron carbide (B_4C) on a tungsten substrate by the chemical vapor deposition from a BCl_3–H_2–CH_4 gas mixture was achieved. An impinging-jet reactor was used to minimize the mass-transfer limitations on the reaction kinetics, which made a detailed kinetic investigation possible. Results of the XRD and XPS analyses showed that the solid product formed on the substrate is a rhombohedral B_4C phase. Both dichloroborane and boron carbide formation rates were found to increase with an increase in the inlet molar fraction of BCl_3. The formation rate of boron carbide increased with an increase in the inlet molar fraction of CH_4. However, no effect on the formation rate of dichloroborane was observed with an increase in the inlet molar fraction of methane. The activation energy of the boron carbide formation reaction was ascertained to be 56.1 ± 4.0 kJ/mol. The boron carbide formation reaction was proportional with the 0.34 ± 0.055 power of the initial boron trichloride concentration and 0.64 ± 0.084 power of the initial methane concentration. © 2006 American Institute of Chemical Engineers *AIChE J,* 52: 4161–4166, 2006

Keywords: chemical vapor deposition (CVD), boron carbide, refractory fibers, hard coatings, jet impingement

Introduction

Refractory fibers are used at temperatures in excess of 1000°C. They are superior to the other fibers with their great durability at high temperatures and by the fact that they have polycrystalline microstructures rather than being amorphous. The majority of fibers of this type are being used for thermal insulation or for advanced composites having the special properties required in aerospace applications. These materials are expensive because they are still manufactured on a small scale. The chief materials of interest are boron, silicon carbide, alumina, and zirconia-based products.[1] Recent materials that are available in fiber form are boron carbide, silicon nitride, and boron nitride.[2] Boron carbide, which is the hardest boron-containing compound after cubic boron nitride, is increasingly gaining importance in the refractory fibers family. Its high melting point, high modulus of elasticity, large neutron capture section, low density, chemical inertness, and outstanding thermal and electrical properties make boron carbide a strong candidate for high technology applications. Boron carbide is a p-type semiconductor material, and because of its convenient band gap (0.77–1.80 eV), it has a potential use in the production of diodes and heterojunctions.[3]

Compared with other refractory materials, such as diamond, silicon carbide, boron nitride, and alumina, relatively little effort has been devoted to the study and development of boron carbide deposition methods. This has started to change in recent years as a result of the need of high-quality boron carbide–based materials, especially in microelectronics, nuclear, military, space, and medical industries.[4] The conventional production methods of boron carbide include the reduction of a boron source, usually boric acid or boric oxide, by carbon above 2000°C. In this high-temperature processes, boron carbide is produced in powder form and an additional sintering process is necessary to produce dense materials.[5] All such complex processes generate some impurities in the final

---

Correspondence concerning this article should be addressed to M. Karaman at kamustaf@metu.edu.tr.

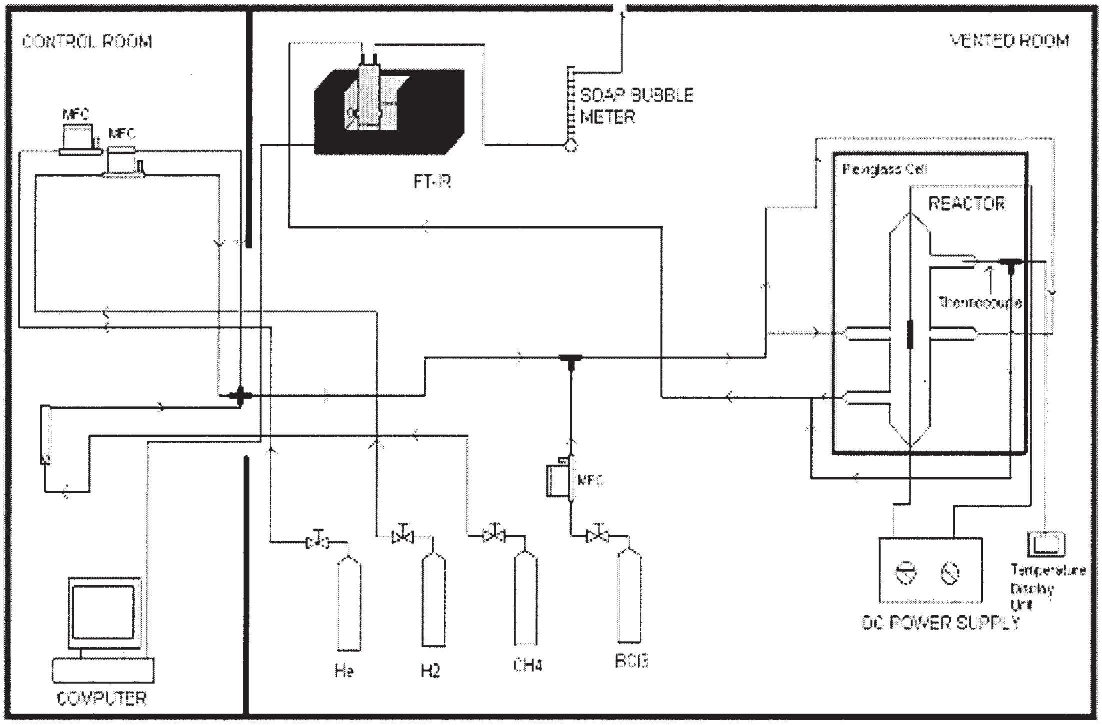

Figure 1. The experimental setup.

product that usually do not permit use of the end product in the high technology applications. On the other hand, the chemical vapor deposition (CVD) method offers the possibility of production of a high-purity boron carbide in the dense form. The CVD processes are widely used in industry because of their versatility for depositing a very large variety of elements and compounds covering a wide range from amorphous deposits to epitaxial layers having a high degree of the perfection and purity.[6] Boron carbide can be deposited on the solid materials (wires, sheets, foils, etc.), which are heated either in a hot wall reactor or in a cold wall reactor by means of the radiofrequency (RF) induction or DC power.

Many investigators have applied various CVD techniques and reaction kinetics together with the study of product morphology.[1,7-9] Vandenbulcke[9] deposited boron carbide from a BCl_3–CH_4–H_2 mixture by using a stagnation flow technique in a cold-wall reactor. The deposition rates and the solid compositions were compared with a mass-transfer equilibrium model. Also deposition domains of the various structures as a function of reaction parameters (the temperature and partial pressures of reaction precursors) were obtained. At various combinations of methane and boron trichloride within excess hydrogen, single-phase boron carbide was obtained over a wide range of temperatures (1400–1900 K). Dilek at al.[8] studied the CVD of B_4C on a tungsten filament from a gas mixture of BCl_3, CH_4, and H_2 in an impinging-jet reactor. Impinging-jet reactors contain tiny orifices to provide very high flow rates for the reactant gases, which then strike vertically as a jet on the substrate surface. The formation of $BHCl_2$ was verified experimentally and a rate expression for the formation of B_4C was proposed. However, the reaction rate expression was based on the boron trichloride molar fraction only, rather than on the concentrations of each species.

A reactant gas mixture usually flows parallel to a substrate in a CVD reactor. In such a reactor, the molecular and thermal diffusions of the reactant gases to the substrate surface play important roles on the deposition rate. The purpose of this work was to study the chemical kinetics in the chemical vapor deposition of boron carbide by using the impinging-jet CVD reactor in which diffusion limitations were minimized. Chemical analysis of the reactor outlet stream was achieved by use of an FTIR spectrophotometer. The resultant deposits were characterized by the X-ray diffraction (XRD) and X-ray photoelectron spectroscopy (XPS) methods.

Experimental

The experimental apparatus is shown in Figure 1. Reactant gases—BCl_3, CH_4, and H_2—were fed to the reactor through the two orifices in the middle of the reactor to provide well impingement onto both sides of the tungsten substrate, which hangs between the two electrodes in the reactor. The diameter of the reactor was 1 cm, whereas the diameters of the orifices were 1 mm each. Distance between the orifices and the substrate surface was 0.5 cm. Electrodes are connected to a DC power supply to heat the tungsten substrate (3 mm wide; 3 cm long) resistively and the applied voltage was continuously regulated. The flow rates of BCl_3 and H_2 gases were controlled by mass flow controllers, whereas the flow rate of methane was adjusted by a rotameter. The piping system in which the gases flow was made up of 1/4-in. brass tubes. The reactor exit stream was connected to the FTIR (Perkin Elmer Spectrum One) for the on-line chemical analysis. The FTIR gas cell temperature was kept at 110°C during the experiments to prevent the condensation of BCl_3 on the mirrors and KBr windows of the cell. The temperature of the substrate surface

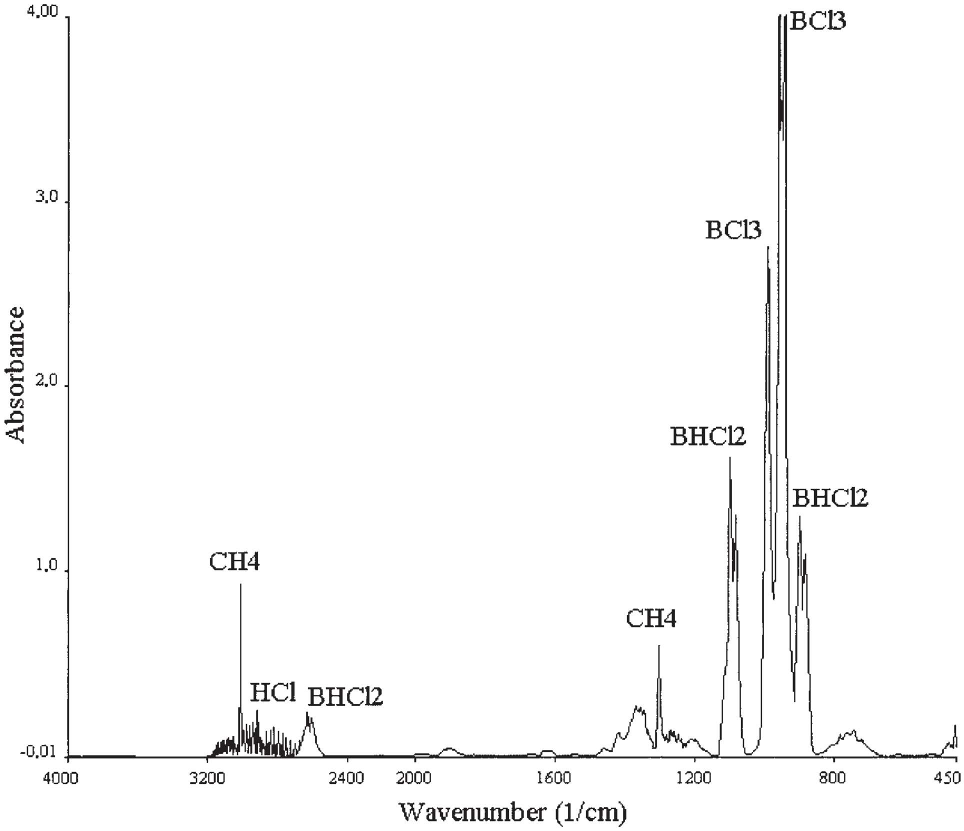

Figure 2. Typical FTIR spectrum of the reactor effluent after heating the substrate.

was measured continuously using an optical pyrometer. The use of quartz as a reactor material provided visual access to the substrate material so that the temperature measurements were made possible. Also, to measure the reactor outlet temperature, a Cr–Ni thermocouple (K-type) was connected to the reactor outlet. Because BCl_3 is a toxic substance, the whole system was built in a continuously ventilated chamber.

The total volumetric flow rate of the gas mixture was kept at 200 cm^3/min and the experiments were carried out at atmospheric pressure. The inlet temperature of the gas mixture was 20°C, whereas the exit temperature was determined to be between 30 and 45°C, depending on the substrate surface temperature. The temperature of the tungsten substrate surface was changed from 1000 to 1400°C to investigate the effect of temperature on reaction kinetics. The temperature of the substrate has a great effect on the structure of the deposited solid phase; the temperature range used for the experiments was selected to favor the production of pure single-phase β-rhombohedral boron carbide. The necessary information for the selection of the temperature range was found according to the deposition domains that were obtained from the literature.[4,9] All experiments were carried out with a methane mole fraction range of 0.019–0.042 and a boron trichloride mole fraction range of 0.023–0.126 in excess hydrogen. In the applied experimental conditions, the reaction system reached steady state within 30–40 min. The solid deposit was analyzed by XRD and XPS for phase and composition identifications, respectively.

Results

The qualitative and quantitative chemical analyses of the reactor effluent stream were performed using FTIR spectroscopy. An FTIR spectrum taken during a typical run is shown in Figure 2. In addition to the characteristic peak groups of the reactant gases (BCl_3, CH_4), the other peaks corresponding to the reaction products ($BHCl_2$, HCl) were also observed.

XRD analysis of the deposit was carried out using a Philips PW 1840 model diffractometer with a Cu–K_α (λ = 1.54 Å) radiation. The diffraction pattern of the solid produced at 1150°C for a process time of 47 min is given in Figure 3. The most intense diffraction peaks were observed at Bragg angle (θ) values of 37.8 and 34.95° with the corresponding hkl values

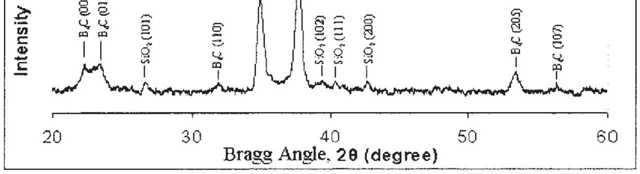

Figure 3. XRD pattern of the solid produced at a temperature of 1150°C and initial composition of 8.1% BCl_3, 1.94% CH_4 in hydrogen.

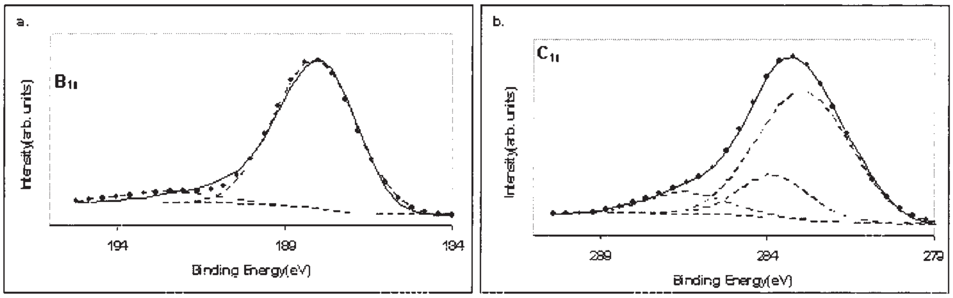

Figure 4. (a) B_{1s} and (b) C_{1s} core levels taken from the XPS spectra of the produced solid phase together with spectrum deconvolution and Shirley background.

Experimental data (solid lines), deconvoluted components (dashed lines), and fitted results (dots).

of 021 and 104, respectively, which are the major XRD peaks of the technical-grade rhombohedral $B_{12}C_3$ stoichiometry (JCPDS 35-0798).[10] There are also diffraction peaks at Bragg angles of 22.0, 23.5, 31.9, 53.5, and 56.55°, with the corresponding hkl values of 003, 012, 110, 205, and 107, which also belong to the rhombohedral boron carbide phase. In addition to the rhombohedral boron carbide phase, the SiO_2 phase is observed at diffraction angles of 26.65, 39.46, 40.55, and 42.46° with the corresponding reflection values of 101, 102, 111, and 200, respectively (JCPDS 33-1161).[10] Existence of the SiO_2 phase is expected, given that the samples were made powder in a pestle made of quartz, which may possibly be scraped into the powder by harder boron carbide particles.

Similar diffraction patterns were obtained for the solid deposits produced at different temperatures. Analysis of the solid deposit revealed that the solid product formed on the tungsten substrate is a rhombohedral B_4C phase. In other words, the occurrence of any phase other than boron carbide was never seen in the temperature range studied.

Although the absence of any impurities such as free carbon and boron in the grown phases was verified from the XRD patterns, the sensitivity of XRD analysis may not be sufficient to verify the amounts of such phases. The atomic composition of the product is thus of great importance. For this reason, XPS analyses were carried out with a monochromatic Mg–K_α (hw = 1253.6 eV) radiation using a Specs spectrophotometer. The samples were ground to powder and bombarded with 3000 eV Ar^+ ions for 15 min. In Figure 4, the B_{1s} and C_{1s} spectra, obtained with the XPS scan together with the spectrum deconvolution and Shirley background, are presented. The deconvolution for the B_{1s} spectrum (Figure 4a) shows the existence of the two possible boron chemical states with binding energies centered at 188.3 and 192.4 eV. The chemical state centered at 188.3 eV binding energy is attributed to B—C bonds in B_4C and the small component centered at 192.4 eV is assigned to boron atoms bonded to oxygen.[11] There is no indication of the existence of any free boron atoms. The deconvolution results for the C_{1s} peak are given in Figure 4b. The spectrum has a shoulder on the left-hand side, which is a result of the oxyboron carbide species at binding energy values of 286.4 and 283.8 eV for C═O and C—O, respectively.[12,13] The large dominating peak centered at the binding energy value of 282.9 eV is attributed to carbon bonded to boron in the carbide phase (in B_4C form). Free carbon, either in graphitic or in diamond phase, is not observed according to the deconvolution results. Boron carbide exists as a single stable phase with a homogeneity range of 8 to 20 atomic % carbon concentration.[4] In the XPS analysis, quantification of the obtained spectra of the sample produced at 1150°C showed a carbon ratio of 17.2 at. %, which is in the homogeneity range of the single stable phase of boron carbide. The XPS spectra do not indicate any other phases besides the boron carbide phase.

From analyses of the FTIR and XPS spectra and XRD patterns it was concluded that the two major independent overall reactions should be considered for the CVD of boron carbide[8,9]:

Reaction 1

$$BCl_3(g) + H_2(g) + 1/4CH_4(g) \Rightarrow 1/4B_4C(s) + 3\,HCl(g)$$

Reaction 2

$$BCl_3(g) + H_2(g) \Rightarrow BHCl_2(g) + HCl(g)$$

Designating the conversion of BCl_3 to boron carbide as x_1 and to dichloroborane as x_2, the mole fractions of reactor effluent gases are expressed in terms of x_1 and x_2 as follows:

$$y_{BCl_3} = \frac{y_{BCl_{3o}}(1 - x_1 - x_2)}{1 + 3/4y_{BCl_{3o}}x_1} \tag{1}$$

$$y_{CH_4} = \frac{y_{CH_{4o}} - 1/4y_{BCl_{3o}}x_1}{1 + 3/4y_{BCl_{3o}}x_1} \tag{2}$$

$$y_{H_2} = \frac{y_{H_{2o}} - y_{BCl_{3o}}(x_1 + x_2)}{1 + 3/4y_{BCl_{3o}}x_1} \tag{3}$$

$$y_{HCl} = \frac{y_{BCl_{3o}}(3x_1 + x_2)}{1 + 3/4y_{BCl_{3o}}x_1} \tag{4}$$

$$y_{BHCl_2} = \frac{y_{BCl_{3o}}x_2}{1 + 3/4y_{BCl_{3o}}x_1} \tag{5}$$

From the experimental data of product and reactant stream compositions the fractional conversions x_1 and x_2 were evaluated from Eqs. 1 and 2. To verify the material balance around

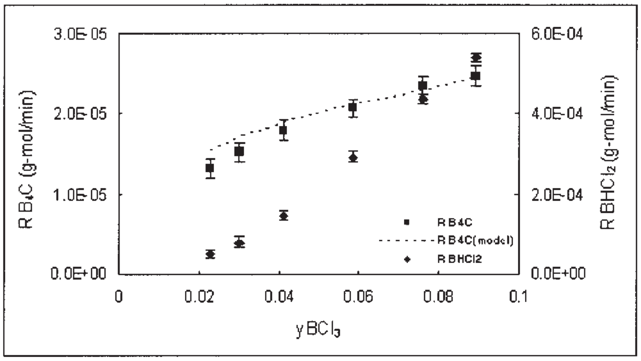

Figure 5. Effect of the initial BCl_3 mole fraction on the B_4C and $BHCl_2$ formation rates.

T = 1150°C, $y_{CH_{4o}} = 0.02$ in hydrogen, $y_{BCl_{3o}}/y_{CH_{4o}}$ = 1.5–5.5.

the reactor, the experimental values of HCl and $BHCl_2$ mole fractions were compared with calculated values using Eqs. 4 and 5. Experimental and calculated values were determined to be the same. Boron carbide deposition and dichloroborane formation rates were evaluated from these mole fractions and the relations between the reaction rates (R):

$$R_{B_4C} = A(R_{B_4C})_s = 1/4F_o y_{BCl_{3o}} x_1 \tag{6}$$

$$R_{BHCl_2} = A(R_{BHCl_2})_s = F_o y_{BCl_{3o}} x_2 \tag{7}$$

where F_o is the total molar flow rate of the reactant stream and A is the surface area of the tungsten substrate that is in contact with the reactant gases within the reactor.

The boron carbide formation rate was also determined from the weight change of the filament during the reaction. The reaction rates calculated from weight change of the filament and from analysis of the reactor exit gases were in substantial agreement, which also demonstrated that the two independent reactions (Reactions 1 and 2) are sufficient to describe the reaction system under consideration.

Effects of the initial boron trichloride mole fraction on the reaction rates were analyzed by varying the boron trichloride molar fraction in the inlet stream between 2.3 and 12.6%. In these experiments, the mole fraction of methane in the reactor inlet stream was kept constant near 2%, and the rest was excess hydrogen, which summed up to a total molar flow rate of 200 cm^3/min.

Changes in the mole fraction of hydrogen in the inlet gas mixture, in the range of 85–95%, seemed to have no effect on the reaction kinetics. Low hydrogen concentrations in the inlet gas resulted in carbon deposition rather than B_4C formation. The effect of inlet BCl_3 concentration on the reaction rates at a temperature of 1150°C can be seen in Figure 5, which indicates that both the reaction rate and the conversion for the boron carbide formation reaction are always lower than those for the dichloroborane formation reaction. Dichloroborane formation reaction is believed to occur in the thin boundary layer next to the substrate surface. This may be the reason for the higher production rates of dichloroborane than those of boron carbide, which occur only through surface reactions. The rate of boron carbide formation reaction increases with an increase in BCl_3 inlet molar fraction, showing a decreasing trend in the slope at high BCl_3 inlet mole fractions. The rate of reaction seemed to be controlled by surface kinetics. The rate of dichloroborane formation reaction is fast enough to consume the excess amount of BCl_3 at high inlet concentrations of BCl_3 and increases with an increase in BCl_3 inlet molar fraction.

In Figure 6, the temperature dependency of B_4C and $BHCl_2$ formation rates is given; one can observe that the boron carbide formation rate increases continuously with temperature. With increasing temperature, the rate of dichloroborane formation reaction also increases; however, the change is not significant compared with the effect of temperature on the formation rate of B_4C. With a change of substrate temperature from 1000 to 1400°C, the rate of B_4C deposition increases almost fourfold, whereas the rate of $BHCl_2$ formation increases around 1.05-fold. This further supports the idea of gas-phase formation of dichloroborane in the boundary region next to the substrate surface. It may be expected that a change in surface temperature in this impinging-jet system may have a smaller effect on the vapor-phase kinetics and thus less impact on the reaction rates compared with the solid-phase kinetics in the formation of boron carbide. It is also seen that the reaction rate for boron carbide formation reaction is lower than that of dichloroborane formation reaction over the entire range of temperatures studied. The effects of methane concentration in the inlet stream on the reaction rates were analyzed by changing the methane mole fraction in the inlet stream in the range of 1.9–4.2%; the results are depicted in Figure 7. The change of methane mole fraction in the inlet stream has almost no effect on the reaction rate of dichloroborane formation reaction over the composition range of methane that was applied during the runs. However, there is an increasing trend in the rate of boron carbide formation reaction.

Experimental data, collected in the given ranges of inlet composition and temperature, were used to determine a reaction rate expression for the formation of B_4C. All data points were placed in an Arrhenius type of reaction rate expression, as follows:

$$R_{B_4C} = k_o \exp(-E_a/RT)[BCl_3]^a[CH_4]^b$$

By use of a computerized nonlinear model-fitting procedure, the experimental data were tested to ascertain the model pa-

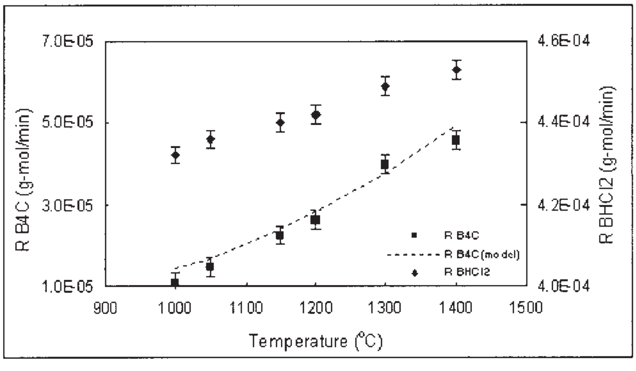

Figure 6. Effect of the substrate temperature on the B_4C and $BHCl_2$ formation rates.

$y_{BCl_{3o}} = 0.081$, $y_{CH_{4o}} = 0.02$, in hydrogen.

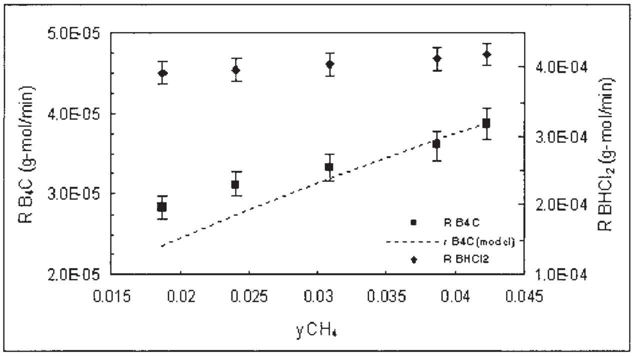

Figure 7. Effect of the initial CH_4 mole fraction on the B_4C and $BHCl_2$ formation rates.

T = 1150°C, $y_{BCl_{3o}} = 0.084$ in hydrogen, $y_{BCl_{3o}}/y_{CH_{4o}} = 2–4.5$.

rameters. The iteration method introduced by Hooke and Jeeves[14] was used for analysis of the data. After the analysis, the frequency factor k_o and activation energy E_a were determined to be 0.078 ± 0.008 and 56.1 ± 4.0 kJ/mol, respectively. The order of reaction with respect to BCl_3 was 0.34 ± 0.055, whereas the order with respect to CH_4 was 0.64 ± 0.084, with a statistical correlation coefficient of 0.97.

Conclusions

The XRD and XPS analyses of the samples produced under different process conditions revealed the existence of a β-rhombohedral boron carbide phase in the deposits. In all of the conducted experiments, the rate of boron carbide formation reaction was always lower than that of the dichloroborane formation reaction. Both rates increase with an increase in the inlet molar fraction of boron trichloride, although the B_4C formation rate stabilizes at high BCl_3 inlet concentrations. This implies that the boron carbide formation reaction may be surface reaction limited at that temperature. All the collected kinetic data were fit in an Arrhenius type of a model equation and the activation energy was found to be 56.1 ± 4.0 kJ/mol. The observed correlation coefficient value after the nonlinear regression analysis was 0.97, which actually needs to be improved by assigning more realistic rate equations that are usually applied for catalytic reactions. This is possible only by a detailed kinetic modeling study.

Acknowledgments

The authors thank the Scientific and Technological Research Council of Turkey (TUBITAK) (Project No. Misag-217) and State Planning Organization of Turkey (Project No. BAP-08-11-DPT2002K120510-IM-5) for financial support of this project.

Notation

A = reaction surface area, mm^2
E_a = activation energy, kJ/mol
F_o = molar flow rate of the reactant stream, mol/min
k_o = frequency factor, mol/min
R = gas constant, kJ mol^{-1} K^{-1}
R_s = reaction rate based on the unit surface area of the substrate, mol min^{-1} mm^{-2}
R = reaction rate based on the surface area of the filaments, mol/min
T = temperature, K
x_1 = fractional conversion of BCl_3 to B_4C
x_2 = fractional conversion of BCl_3 to $BHCl_2$
y_i = mole fraction of component i

Literature Cited

1. Grigor'ev YM, Shugaev VA, Mukas'yan AS, Samoilenko NG, Shiryaev AA. The chemical vapor deposition of boron carbide from a BCl_3–C_7H_8–H_2 mixture onto heated support. *Russ J Inorg Chem.* 1991;36:1089-1091.
2. Chlorophenols to copper compounds. *Ullmann's Encyclopedia of Industrial Chemistry*. 5th Edition. Mississauga, Ontario, Canada: John Wiley & Sons Canada Ltd.; 1986:Vol. A7.
3. Byun D, Spady BR, Ianno NJ, Dowben PA. Comparison of different chemical vapor deposition methodologies for the fabrication of heterojunction boron-carbide diodes. *Nano Struct Mater.* 1995;5:465-471.
4. Sezer AO, Brand JI. Chemical vapor deposition of boron carbide. *Mater Sci Eng*. 2001;B79:191-202.
5. Thevenot F. Boron carbide—A comprehensive review. *J Eur Ceram Soc.* 1990;6:205-225.
6. Bunshah RF. *Handbook of Hard Coatings*. Park Ridge, NJ: Noyes Publications; 2001.
7. Ploog K. Composition and structure of boron carbides prepared by CVD. *J Crystal Growth.* 1974;24/25:197-204.
8. Dilek SN, Özbelge HÖ, Sezgi NA, Doğu T. Kinetic studies for boron carbide in a dual impinging-jet reactor. *Ind Eng Chem Res.*2001;40: 751-5.
9. Vandenbulcke LG. Theoretical and experimental studies on the chemical vapor deposition of boron carbide. *Ind Eng Chem Res.* 1985;24: 568-575.
10. *Selected Powder Diffraction Data for Education and Training Search Manual*. Newtown Square, PA: International Centre for Diffraction Data; 1988:Vols. 1 and 2.
11. Pan WJ, Sun J, Ling H, Xu N, Ying ZF, Wu JD. Preparation of thin films of carbon-based compounds. *Appl Surf Sci.* 2003;218:297-304.
12. Jacobsohn LG, Schulze RK, Maia da Costa MEH, Nastasi M. X-ray photoelectron spectroscopy investigation of boron carbide films deposited by sputtering. *Surf Sci.* 2004;572:418-424.
13. Lee KE, Lee JY, Park MJ, Kim JH, Lee CB, Kim CO. Preparation of boron carbide thin films for HDD protecting layer. *J Magn Magn Mater*. 2004;272-276:2197-2199.
14. Hooke R, Jeeves TA. Direct search solution of numerical and statistical problems. *J Assoc Comput Machinery*. 1961;8:212-229.

Manuscript received Mar. 19, 2006, and revision received Aug. 23, 2006.